

## Paper

Int'l J. of Aeronautical & Space Sci. 17(1), 101–108 (2016)  
DOI: <http://dx.doi.org/10.5139/IJASS.2016.17.1.101>

**IJASS**  
International Journal of  
Aeronautical and Space Sciences

# RCS Numerical Simulation of Stealth Modified Three-Surface Aircraft

**Cheng Liangliang\***

*School of Aeronautic Science and Engineering, Beijing University of Aeronautics and Astronautics, Beijing 100191, China.  
Department of Airborne Vehicle Engineering, Naval Aeronautical and Astronautical University, Yantai 264001, China  
Department of Carrier-based Engineering, Naval Aviation Institute, Huludao 125001, China*

**Yue Kuizhi\*\***

*Department of Airborne Vehicle Engineering, Naval Aeronautical and Astronautical University, Yantai 264001, China*

**Xing CuiFang\*\*\***

*Department of Basic Sciences, Naval Aeronautical and Astronautical University, Yantai 264001, China*

**Yu Dazhao\*\*\*\***

*Department of Airborne Vehicle Engineering, Naval Aeronautical and Astronautical University, Yantai 264001, China*

## Abstract

The RCS characteristics of stealth modified three-surface aircraft are analyzed in this paper. Prototype A is built with CATIA software and the three-dimensional digital models of modified stealth three-surface B and C are also designed based on carrier-based aircraft Su-33; the numerical simulation of RCS characteristics of three-surface aircraft is conducted with RCSAnsys software based on physical optics method and the method of equivalent currents; The following results are obtained by comparative analysis and mathematical statistics: (1) by the use of physical optics method and equivalent electromagnetic current method, the scattering intensity for each part of the model and RCS characteristic of the aircraft can be analyzed efficiently and accurately; (2) compared with model A, the mean RCS value of model B is reduced to 14.1% in forward direction and 48.1% in lateral direction; (3) compared with model A, the mean RCS value of model C decreases to 11.4% in forward direction and 21.6% in lateral direction. The results are expected to provide theoretical basis and technical support to the conceptual design of aircraft and stealth technology research.

**Key words:** aircraft conceptual design, three-surface aircraft, stealth, physical optics method, numerical simulation.

## 1. Introduction

The three-surface aerodynamic configuration which consists of canard wings, the main wings and the tails, is one of the four common aerodynamic configurations of aircrafts together with normal configuration, canard configuration and all-wing configuration. With a high lift-drag ratio, a three-surface aircraft shows good aerodynamic performances, as well as an excellent maneuverability at low speeds and low

levels. There are several types of three-surface configuration operational aircrafts internationally, such as Su-33, Su-34 and Su-37 of Russia, F-15S/MTD of USA and T-2CCV of Japan, etc. Having been in service on carrier Admiral Kuznetsov for more than 20 years, Su-33 is one of the main fighters of the Russian Naval Aviation. It represents the design concept of the 1970s-80s—a focus on aerodynamic performance rather than on stealth. Nowadays the study of stealth of operational aircrafts has attracted more attention.

This is an Open Access article distributed under the terms of the Creative Commons Attribution Non-Commercial License (<http://creativecommons.org/licenses/by-nc/3.0/>) which permits unrestricted non-commercial use, distribution, and reproduction in any medium, provided the original work is properly cited.

© \* Ph. D  
\*\* Ph. D, Corresponding author: [yuekuizhi\\_2000@sohu.com](mailto:yuekuizhi_2000@sohu.com)  
\*\*\* Assistant Professor  
\*\*\*\* Assistant Professor

Received: March 30, 2015 Revised: December 14, 2015 Accepted: December 18, 2015  
Copyright © The Korean Society for Aeronautical & Space Sciences

101

<http://ijass.org> pISSN: 2093-274x eISSN: 2093-2480

The design concept of stealth has been applied to modern operational aircrafts throughout the world, such as B-2, F-22[1], F-35[2], X-45 and X-47 of the USA, Su-47, MG-1.44 and T-50 of Russia, etc. Several issues on stealth have been studied thoroughly by researchers at home and abroad who have discussed radar stealth [3], infrared stealth, visible light stealth and acoustic stealth. They studied material-stealth technology and key technologies of shape-stealth, such as fuselage stealth [4], wing configuration stealth [5], air inlet stealth [6] and surface crack stealth [7]. Some other researchers are also concerned about the issues on RCS models and algorithms. For example, in reference [8], the effect of inner weapons and external weapons on RCS performance is discussed; based on the RCS characteristics of different objects, the synthetically analytical method of stealth characteristics is applied to estimate the performance of the stealth aircraft in reference [9]; the RCS performances of metal cone and the metal cone with plasma covering are numerically simulated in reference [10]; three new controlling factors for multilevel fast multipole algorithm (MLFMA) are proposed in reference [11] to improve the computational efficiency of the algorithm; the integrated computing technology about the identification of the main scattering source of complex objects is studied in reference [12], which provides a suitable solution for large-scale complex objects and cases with low accuracy requirement of RCS; A dimensionality reduction model is built in reference [13] in order to numerically simulate the three-dimensional electromagnetic scattering and estimate the RCS of monostatic radars quickly. The stealth performances and aerodynamic characteristics of a conceptually designed aircraft are discussed in reference [14]. A stealth embarked early warning aircraft and an electronic warfare aircraft are conceptually designed and discussed in reference [15] and reference [16] respectively. In reference [17], an aircraft of variable-sweep wings is conceptually designed and the stealth performance of the aircraft is studied. The stealth characteristics of the typical stealth aircrafts are discussed based on probabilistic method in reference [18]. Although the stealth technology has been over-studied in several respects, certain problems of conceptual design and stealth technology are still overlooked. Neither public academic researches on the RCS characteristics of three-surface aircraft nor the findings on the RCS characteristics of modified stealth operational aircrafts in service have been obtained.

Aiming at the shortcomings mentioned above, the paper builds 3 types of three-dimensional digital models of three-surface aircrafts with CATIA software. Based on physical optics method and equivalent electromagnetic current

method, it numerically simulates the RCS characteristics of the stealth modified three-surface aircraft with self-compiled software RCSAnsys. The mathematical statistics of forward, lateral and backward RCS performances of the aircraft at different pitch angles are also analyzed comparatively in the paper. It is expected that the results of the paper will provide reference bases to aircraft conceptual design and give fundamental support to stealth modification of three-surface aircrafts.

## 2. Testing Algorithm

The theoretical basis of the numerical simulation for the RCS characteristics of stealth modified three-surface aircraft includes RCS testing method, mathematical statistics and unit conversion, and experimental verification.

### 2.1 RCS Testing Method

The physical optics method is applied in the paper to calculate surface element scattering, and the method of equivalent currents is applied to calculate the edge diffraction. The integrated numerical simulation of the RCS characteristics of the aircraft is conducted using the two methods together.

The physical optics solution of RCS based on triangular patch model is shown as below [19]:

$$\sqrt{\sigma_{po}} = \frac{jk}{\sqrt{\pi}} \hat{n} \cdot (\hat{e}_s \times \hat{h}_i) e^{jk(\hat{s}-\hat{i})r_0} I' \quad (1)$$

Where

$$I' = \begin{cases} \frac{e^{jk(\hat{s}-\hat{i})r_m} \sum_{m=1}^3 \mathbf{p} \cdot \mathbf{L}_m \operatorname{sinc}\left(\frac{k(\hat{s}-\hat{i}) \cdot \mathbf{L}_m}{2}\right)}{jk|\mathbf{p}|^2} & |\mathbf{p}| \neq 0, \\ A & |\mathbf{p}| = 0 \end{cases}$$

Where  $\sqrt{\sigma_{po}}$  ( $\text{m}^2$ ) is the RCS of a single patch element;  $j$  is the imaginary unit and  $j^2=-1$ ;  $k=2\pi/\lambda$  is the free space wave beam, where  $\lambda$  (m) is the length of incoming radar wave;  $\hat{n}$  is the unit normal vector of object surface;  $\hat{e}_s$  is the unit vector in the direction of the electromagnetic polarization of receiving antenna;  $\hat{h}_i$  is the unit vector of the direction of the incoming wave field;  $r_0$  is the reference point attached to the patch element definitely;  $\hat{i}$  is the unit vector of the incoming direction;  $\hat{s}$  is the unit vector of scattering direction;  $r_m$  is the vector from reference point  $r_0$  to the midpoint of the  $m$  th edge;  $\mathbf{p} = \hat{n} \times (\hat{s} - \hat{i})$ ;  $L_m$  is the  $m$  th edge and a vector meanwhile;  $\operatorname{sinc}(x) = \frac{\sin(x)}{x}$ ;  $A$  is the area of patch element ( $\text{m}^2$ ).

The expression of equivalent electromagnetic current method is as follows [20, 21]:

$$\sqrt{\sigma_{ecm}} = \frac{1}{\sqrt{\pi} \sin \theta} [(E_o^i \cdot t) f s \times (s \times t) - Z_0 (H_o^i \cdot t) g s \times t] \cdot e^{-j2kr_s} \frac{\sin(kl \cdot s)}{kl \cdot s} \quad (2)$$

where  $\sqrt{\sigma_{ecm}}$  stands for single marginal RCS ( $m^2$ );  $t$  stands for the unit vector on marginal tangent direction;  $\theta$  stands for the intersection angle of incoming line  $i$  and  $t$ ;  $E_o^i$  stands for the incoming electric field intensity (V/m);  $f$  and  $g$  are the Yoffie Rousseff diffraction coefficients;  $Z_0$  stands for the vacuum wave impedance ( $\Omega$ );  $H_o^i$  stands for incoming magnetic field intensity (A/m);  $r_s$  stands for the position vector at the middle of the edge and  $l$  stands for edge vector.

The RCS of the whole aircraft is the sum of RCS of all the  $n$  surface elements and  $m$  edges, the superposition expression is as follows:

$$\sigma = \left| \sum_{i=1}^n (\sqrt{\sigma_{po}})_i + \sum_{j=1}^m (\sqrt{\sigma_{ecm}})_j \right|^2 \quad (3)$$

## 2.2 Mathematical Statistics and Unit Conversion

$$\bar{\sigma}_{\theta_r}^{n-N} = \frac{1}{N-n+1} \sum_{\psi_r=n}^N \sigma_{\theta_r}^{\psi_r} \quad (4)$$

$$\sigma_{dBm^2} = 10 \lg \sigma \quad (5)$$

where  $\sigma_{\theta_r}^{\psi_r}$  is the RCS value ( $m^2$ ) where incoming wave pitch

angle is  $\theta_r$  and azimuth angle is  $\psi_r$ ;  $\bar{\sigma}_{\theta_r}^{n-N}$  is the arithmetic mean value where the incoming wave pitch angle is  $\theta_r$  and azimuth angle is  $\psi_r$  ( $\psi_r = n \sim N$ ) ( $m^2$ );  $\sigma$  stands for the RCS of the aircraft ( $m^2$ ) and  $\sigma_{dBsm}$  stands for the RCS of the aircraft (dBm<sup>2</sup>).

## 2.3 Experimental Verification

Experimental verification on the effectiveness of the combined method of physical optics and equivalent current for aircraft RCS calculation is conducted by the research group, and the numerical simulation results are published in relative papers, shown in reference [22].

## 3. RCS Characteristic Analysis of the Aircraft

The RCS characteristic analysis of aircraft consists of three parts: the conceptual design of the aircraft, the numerical simulation of the RCS characteristics of the prototype aircrafts and the comparative analysis of the RCS characteristics of stealth modified aircrafts.

### 3.1 Aircraft Conceptual Design

In this section, the three-dimensional digital model of three-surface aircraft is conceptually designed in CATIA software based on carrier-based aircraft Su-33 of Russia. There are three types of models: A, B and C (see Fig.1), where Type A is the prototype aircraft, B and C are stealth modified aircraft, of which the basic size data is shown in Table 1.

Table 1. Basic size data of the three-surface aircraft

item	set value		
	Type A	Type B	Type C
length ( $m$ )	20.795	19.82	22.048
wing span ( $m$ )	14.7	14.7	16.764
leading edge sweepback angle of the main wing ( $^\circ$ )	45	45	42
chord length at blended wing body ( $m$ )	5.5	5.5	5.8
tip chord length of the main wing ( $m$ )	2	2	2
cathedral angle of the main wing ( $^\circ$ )	0	2	2
airfoil profile of the main wing	NACA 64a204	NACA 64a204	NACA 64a204
leading edge sweepback angle of the canard wing ( $^\circ$ )	45	45	42
root chord length of the canard wing ( $m$ )	1.54	1.54	2
tip chord length of the canard wing ( $m$ )	0.42	0.42	0.817
cathedral angle of the canard wing ( $^\circ$ )	7	7	12
airfoil profile of the canard wing	NACA64a202	NACA64a202	NACA64a202
leading edge sweepback angle of the horizontal tail ( $^\circ$ )	45	45	42
root chord length of the horizontal tail ( $m$ )	2.915	2.915	2.915
tip chord length of the horizontal tail ( $m$ )	1.141	1.141	1.141
airfoil profile of the horizontal tail	NACA64a003	NACA64a003	NACA64a003

Type A, a supersonic strike fighter with a single seat, double engines and three-surface configuration, has a straight air inlet, flying tails, fore flaps and trailing edge flaperons. There are rudders on twin vertical fin. The bubble canopy is plated with metallic coating, and the weapons are mounted externally.

Type B is stealth modified based on Type A through the following main measures: (1) the twin vertical fins symmetrically incline at an angle of 35° outward; (2) the nose cross section is modified from round to edged shape and the airspeed head is cancelled; (3) There is a stealth protective screening at the air inlet that can open as required during a low speed flight mission.

Type C is quite different from Type A and the main modifications are as follows: (1) the canard wings, the main wings and the horizontal tails remain; (2) the twin vertical fins are modified into all-moving fins and symmetrically incline at an angle of 35° outward; (3) the nose cross section is modified from round to edged shape and the airspeed head is cancelled; (4) the straight air inlet is modified to diverterless supersonic inlet (DSI); (5) the external weapons are changed into internal weapons.

Model B is a primary stealth modified type of model A. The modified type could be conducted by the industry sector without much difficulty and the stealth performance can be improved by one order of magnitude;

Model C is an advanced stealth modified type of model A. It would take more efforts to be accomplished while the stealth performance of the aircraft could get an increase of two orders of magnitude.

The three-surface aircraft performs well at both high velocity and low velocity. It is suitable for the demands of low altitude and low velocity of the ski-jump takeoff and meets the requirements of combat performance at high velocity and high altitude. The discussion on stealth modified aircraft based on three-surface aircraft can benefit China's embarked stealth aircraft study in the current national situation.

The main purpose of the modifications is to reduce the

RCS in the front sector while other directions of RCS are also considered.

The inlets and nozzles of the aircraft are built in approximate process.

(a) The inlet model of type A: the engines which are considered as cones and circle cylinders are placed in the inlets.

(b) The inlet model of type B: a reticulate inlet protective shield which is assumed as a plate is set at the entrance of the inlet. The functions of the protective shield are to keep the engine away from the suction of sand and hide the engine from the detective radar waves.

(c) The inlet model of type C: it is designed as a DSI inlet, so the entrance of the inlet is sealed just by a curved surface.

(d) The nozzles of type A, B and C: the part from the cone of afterburner to the end of the nozzle is considered as a closed surface. The blades are not included.

The weapon configurations of type A and B are external mounting while that of type C is inner weapon bay.

### 3.2 Numerical Simulation of the RCS Characteristics of the Prototypes

The RCS characteristics of the models are numerically simulated in the self-compiled software RCSAnsys[15,16] under the conditions of incoming wave pitch angle from -10° to +10° and X radar band and H-H polarization based on

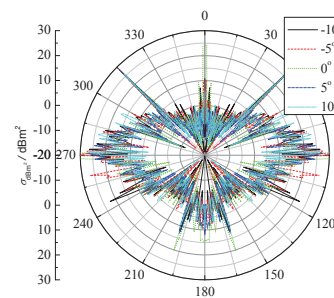


Fig. 2. The RCS characteristic of Type A at various pitch angles

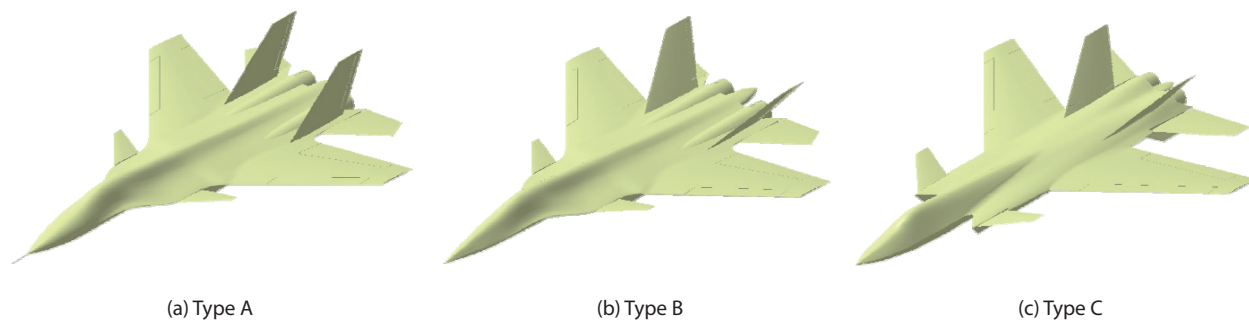


Fig. 1. Three types of three-surface aircraft CATIA models

physical optics method and the method equivalent currents. The RCS curves are obtained and shown in Fig. 2 and the scattering intensity distributions of the models at various azimuth angles are obtained in Fig. 3.

Figure 2 shows that the mean RCS values of Type A at  $\pm 30^\circ$  azimuth angles, X radar band and H-H polarization condition through expressions (4) and (5) are as follows: (1) the forward, lateral and backward mean RCS values are  $-3.901 \text{ dBm}^2$ ,  $15.817 \text{ dBm}^2$  and  $2.826 \text{ dBm}^2$  when the pitch angle is  $10^\circ$ ; (2) the forward, lateral and backward mean RCS values are  $-2.502 \text{ dBm}^2$ ,  $15.817 \text{ dBm}^2$  and  $5.294 \text{ dBm}^2$  when the pitch angle is  $5^\circ$ ; (3) the forward, lateral and backward mean RCS values are  $12.310 \text{ dBm}^2$ ,  $24.687 \text{ dBm}^2$  and  $9.805 \text{ dBm}^2$  when the pitch angle is  $0^\circ$ ; (4) the forward, lateral and backward mean RCS values are  $-0.839 \text{ dBm}^2$ ,  $20.206 \text{ dBm}^2$  and  $3.042 \text{ dBm}^2$  when the pitch angle is  $-5^\circ$ ; (5) the forward, lateral and backward mean RCS values are  $0.214 \text{ dBm}^2$ ,  $16.232 \text{ dBm}^2$  and  $2.090 \text{ dBm}^2$  when the pitch angle is  $-10^\circ$ ;

Figure 3 shows the RCS scattering intensity characteristic of various parts of Type A as follows: (1) the forward RCS scattering intensity is high at the air inlet, radome and canopy; (2) the lateral RCS scattering intensity is high at the vertical fins, air inlet side board and fuselage; (3) The backward RCS scattering intensity is high at the nozzles and tail cone.

The RCS characteristics of stealth modified aircraft are then analyzed after the analysis of Type A.

### 3.3 A Comparative Analysis of the RCS Characteristic of the Stealth Modified Aircraft

The RCS numerical simulations of the three-surface aircraft Type A, B and C are conducted in the article under the following initial conditions: H-H polarization condition, X, S and UHF radar band, incoming wave pitch angles of  $-10^\circ$ ,  $-5^\circ$ ,

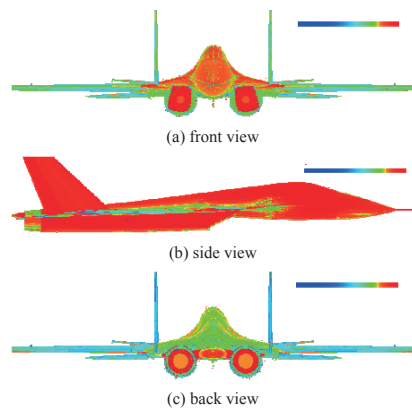


Fig. 3. The RCS scattering intensity of Type A

$0^\circ$ ,  $5^\circ$  and  $10^\circ$ , aircraft azimuth angles from  $0^\circ$  to  $360^\circ$ , circular cone section of the calculating section. A total of 45 curves of RCS characteristics and 16,200 pictures of RCS scattering intensity are obtained through RCS numerical simulations of the three types.

The calculating frequency of UHF band is 0.5GHz; those of S band and X band are 3GHz and 10GHz respectively.

The RCS characteristic curves of stealth modified aircrafts of Type B and C are obtained through numerical simulation in RCSAnsys software in H-H polarization condition, at X radar band and various incoming wave pitch angles. (see Fig. 4) The analysis table of the mean RCS values of Type A, B and C is obtained through mathematical statistics and unit conversion. (see Table 2) The RCS scattering intensity analysis of the three types at various parts is shown in Fig. 5.

Figure 4(a) shows that in H-H polarization condition, at X radar illumination band and in  $\pm 30^\circ$  azimuth angle sector, the mean RCS values of Type B are as follows: (1) the mean forward, lateral and backward RCS value are  $-2.265 \text{ dBm}^2$ ,  $21.481 \text{ dBm}^2$  and  $7.240 \text{ dBm}^2$  where the pitch angle is  $0^\circ$ ; (2) The mean forward, lateral and backward RCS values are gathered in Table 2 when pitch angles are  $10^\circ$ ,  $5^\circ$ ,  $-5^\circ$  and  $10^\circ$  respectively.

Figure 4(b) shows that in H-H polarization condition, at X radar illumination band and in  $\pm 30^\circ$  azimuth angle sector

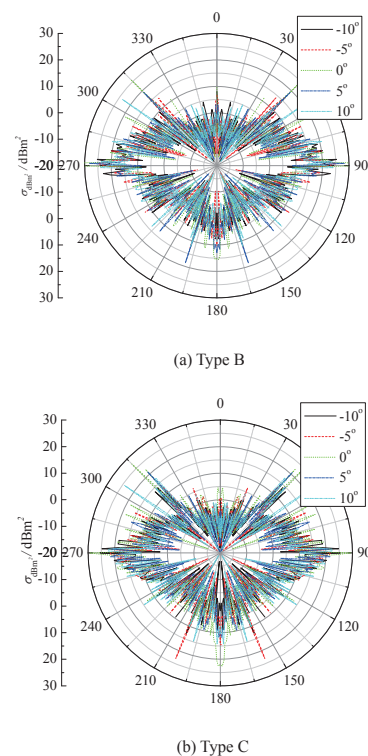


Fig. 4. The RCS characteristic curve of stealth modified aircraft



the mean RCS values of Type C are as follows: (1) the mean forward, lateral and backward RCS value is are  $-1.579 \text{ dBm}^2$ ,  $15.507 \text{ dBm}^2$  and  $12.772 \text{ dBm}^2$  where the pitch angle is  $0^\circ$ ; (2) The mean forward, lateral and backward RCS values gather in Table 2 when pitch angles are  $10^\circ$ ,  $5^\circ$ ,  $-5^\circ$  and  $10^\circ$  respectively.

Table 2 shows that at X radar band and in  $-10^\circ \sim +10^\circ$  pitch angle range the mean RCS values of the aircraft are as follows: (1) the mean RCS values of Type A are about  $5.991 \text{ dBm}^2 = 3.973 \text{ m}^2$  in the front sector,  $20.149 \text{ dBm}^2$  in side sector and  $5.681 \text{ dBm}^2$  in back sector; (2) the mean RCS values of Type B are about  $-2.505 \text{ dBm}^2 = 0.561 \text{ m}^2$  in the front sector,  $5.052 \text{ dBm}^2$  in side sector and  $5.681 \text{ dBm}^2$  in back sector; (3) the mean RCS values of Type C are about  $-3.435 \text{ dBm}^2 = 0.453 \text{ m}^2$  in the front sector,  $13.503 \text{ dBm}^2$  in side sector and  $4.816 \text{ dBm}^2$  in back sector; the results above show that, at X wave band and  $-10^\circ$  to  $+10^\circ$  pitch angles: (1) compared with Type A, the mean RCS values of Type B in the front, side and back sectors decrease to 14.1%, 48.1% and 86.51% respectively; (2) compared with Type A, the mean RCS values of Type C in the front, side and back sectors decrease to 11.4%, 21.6% and 81.9% respectively.

Similarly, the mean RCS characteristics of the three types in S and UHF band are obtained.

Figure 5 (a) and Fig. 5(b) show the comparison between Type B and Type A: (1) the forward RCS scattering intensity of Type B is greatly reduced for the removal of the pitot tube and the installation of the stealth protective screening at the air inlet; (2) the lateral RCS scattering intensity of Type B

is greatly reduced when the nose cross section is modified from round to edged shape and the twin vertical fins symmetrically incline  $35^\circ$  outward.

From Fig. 5(a) and 5(c), compared with Type A, Type C: (1) is weaker in RCS scattering in the forward sector because of the removal of the pitot tube and the installation of DSI inlet; (2) is weaker in RCS scattering in the lateral sectors because of its  $35^\circ$  twin vertical fins and edged shape changed from round; (3) is equal in RCS scattering intensity whether mounted with weapons or not because it has internally mounted weapons.

The reason for the emphasis on X band is that the fire control radar of the fighter uses X band. Air battles are the primary operations of the fighters, so the X band is appreciated in the paper. The UHF band is suitable for radars on early warning aircrafts while S band is for the shipborne aerial search radars, both of them are very important. The research process of UHF band and S band is consistent with that of X band and is described briefly in the paper.

To conclude from Fig. 5 and Table 2, the characteristics of stealth modified 3-surface aircraft are: (1) Type B has improved stealth performance after being adapted from Type A by reducing three RCS characteristics, but it cannot carry internal missiles and will not be stealth at high flight altitude with external weapons. Therefore Type B is suitable for carrying on long-range anti-ship missions at low altitude and low speed; (2) Type C, a better modified three-surface stealth aircraft with internal weapon bay, is dramatically

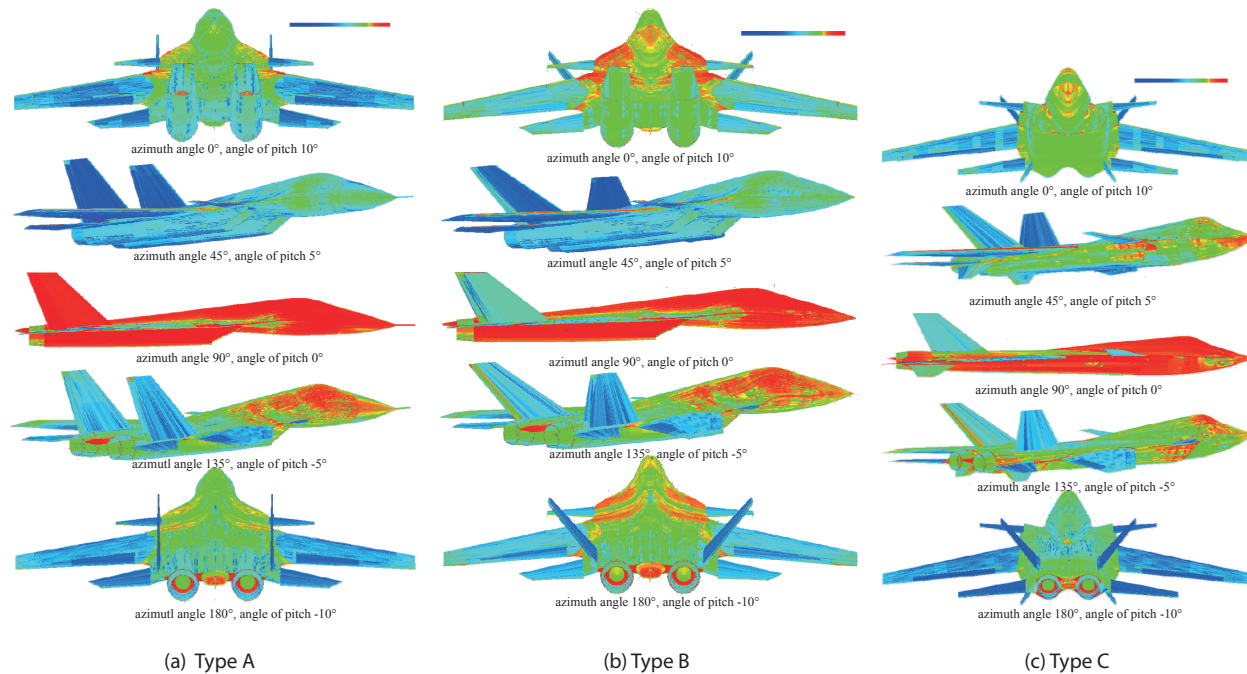


Fig. 5. The comparison of RCS scattering intensity of the aircrafts

Table 2. the mean RCS values of the aircraft in H-H polarization condition

type	band	pitch angle	mean RCS value in the $\pm 30^\circ$ azimuth sector (dBm <sup>2</sup> )		
			front	side	back
A	X	10°	-3.901	15.817	2.826
A	X	5°	-2.502	15.817	5.294
A	X	0°	12.310	24.687	9.805
A	X	-5°	-0.839	20.206	3.042
A	X	-10°	0.214	16.232	2.090
A	S	10°	-4.627	14.791	0.817
A	S	5°	5.235	17.552	4.363
A	S	0°	14.829	25.994	12.497
A	S	-5°	4.038	15.147	5.100
A	S	-10°	-1.263	14.377	-1.063
A	UHF	10°	-12.884	14.525	-3.288
A	UHF	5°	-3.552	18.425	-1.767
A	UHF	0°	3.856	22.182	3.553
A	UHF	-5°	0.137	18.314	-0.993
A	UHF	-10°	-5.710	16.856	-2.020
B	X	10°	-2.996	14.170	3.578
B	X	5°	-3.922	14.051	6.797
B	X	0°	-2.265	21.481	7.240
B	X	-5°	-2.858	13.828	3.777
B	X	-10°	-1.027	15.108	1.000
B	S	10°	-3.180	12.021	0.403
B	S	5°	-3.970	12.454	4.841
B	S	0°	-4.981	15.254	12.544
B	S	-5°	-3.521	14.007	5.231
B	S	-10°	-1.322	12.926	0.281
B	UHF	10°	-9.601	10.733	-3.192
B	UHF	5°	-11.640	12.310	-2.173
B	UHF	0°	-11.944	14.103	3.764
B	UHF	-5°	-6.566	12.718	-0.320
B	UHF	-10°	-5.334	15.290	-1.964
C	X	10°	-5.006	12.569	3.246
C	X	5°	-5.510	11.882	4.949
C	X	0°	-1.579	15.507	6.772
C	X	-5°	-2.046	12.595	4.949
C	X	-10°	-4.557	13.947	3.094
C	S	10°	-3.220	11.904	2.800
C	S	5°	-5.246	11.058	5.652
C	S	0°	-2.414	11.261	9.024
C	S	-5°	-2.617	11.058	9.478
C	S	-10°	-3.113	10.315	3.872
C	UHF	10°	-7.038	6.753	-3.093
C	UHF	5°	-10.14	4.971	-1.878
C	UHF	0°	-9.723	5.787	2.915
C	UHF	-5°	-8.640	7.037	-1.279
C	UHF	-10°	-7.246	8.812	-0.291

improved in stealth operational performance. Therefore, it is suitable for carrying on stealth operations at a middle-altitude and a high speed with middle-range anti-ship missiles or middle-range air-to-air missiles.

#### 4. Conclusion

Based on physical optics method and the method of equivalent currents, this research analyses the RCS characteristics of three-surface aircraft. A numerical simulation is conducted to analyze the RCS characteristics and scattering intensities in different sectors of Type A, B and C three-surface aircrafts, using the self-programmed software RCSAnsys.

The following conclusions are reached:

- (1) Physical optics method and the method of equivalent currents can be used to analyze the scattering intensity of each part and the RCS characteristics of the aircraft efficiently and accurately;
- (2) Type B and C stealth aircraft, reconfigured from Type A three-surface aircraft, show much lower mean RCS values in the forward, lateral and backward sectors on X, S and UHF bands.

#### Acknowledgement

This work was supported by the Natural Science Foundation of China (51375490).

## References

- [1] Suresh, R.P. and Christopher, L.B., "F/A-22 Vertical Tail Buffet Strength Certification," *AIAA 2005-2292*.
- [2] Paul, M.B., "Genesis of the F-35 Joint Strike Fighter," *Journal of Aircraft*, Vol. 46, No. 6, 2009, pp. 1825-1836.
- [3] Sun, C. and Zhang, P., "Lo Requirements and Solutiona of Avionics/RF System for Advanced Aircraft," *Acta Aeronautica et Astronautica Sinica*, Vol. 29, No. 6, 2008, pp. 1472-1481.
- [4] Bai, Z.D., Liu, H. and Wu, Z., "Param etricm ode ling and optim ization of observability fuselage in aircraft conceptual design," *Journal of Beijing University of Aeronautics and Astronautics*, Vol. 33, No. 12, 2007, pp. 1391-1394.
- [5] Sun, Q. and Tian, W., "Numerical Study of Medium Stealth Scale-down Models for Airfoil Shape," *Acta Aeronautica et Astronautica Sinica*, Vol. 29, No. 3, 2008, pp. 670-674.
- [6] Shi, L. and Guo, R.W., "Electromagnetic Scattering of a Submerged Inlet," *Acta Aeronautica et Astronautica Sinica*, Vol. 29, No. 5, 2008, pp. 1098-1104.
- [7] Huang, P. L. and Liu, Z.H., "Research on Electromagnetic Scattering Characteristics of Slits on Aircraft," *Acta Aeronautica et Astronautica Sinica*, Vol. 29, No. 3, 2008, pp. 675-680.
- [8] Yue, K.Z., Sun, C. and Liu, H., "Numercal simulation on the RCS of combat aircraft for mounted missile," *Systems Enginceering and Electronics*, Vol. 36, No. 1, 2014, pp. 62-67.
- [9] Li, Y., Huang, J. and Hong, S., "A new assessment method for the comprehensive stealth performance of penetration aircrafts," *Aerospace Science and Technology*, Vol. 15, No. 7, 2011, pp. 511-518.
- [10] Shen, S.M.C., "FDTD simulations on radar cross sections of metal cone and plasma covered metal cone," *Vacuum*, Vol. 86, No. 7, 2012, pp. 970-984.
- [11] Liu, Z.H., Huang, P.L. and Gao, X., "Multi-frequency RCS Reduction Characteristics of Shape Stealth with MLFMA with Improved MMN," *Chinese Journal of Aeronautics*, Vol. 23, No. 3, 2010, pp. 327-333.
- [12] Huang, M.J., Lü, M.Y. and Huang, J., "Recognition of the major scattering sources on complex targets based on the high frequency radar cross section integrated calculation technique," *Journal of Shanghai University*, Vol. 13, No. 4, 2009, pp. 115-121.
- [13] Ledger, P.D. and Morgan, K., "An Adjoint Enhanced Reduced-Order Model for Monostatic RCS Computation," *Electromagnetics*, Vol. 28, No. 1, 2008, pp. 54-76.
- [14] Yue, K.Z., Chen, S.C., Liu, W.L. and Yu D.Z., "Simulation of Conceptual Designs of a Three-Surface Stealth Strike Fighter," *International Journal of Aeronautical and Space Sciences*, Vol. 15, No. 4, 2014, pp. 366-373.
- [15] Yue, K.Z., Gao, Y. and Li, G.X., "Conceptual design and RCS performance research of shipborne early warning aircraft," *Journal of Systems Engineering and Electronics*, Vol. 25, No. 6, 2014, pp. 968-976.
- [16] Yue, K.Z., Liu, W.L., Li, G.X. and Ji, J.Z., "Numerical Simulation of RCS for Carrier Electronic Warfare Airplanes," *Chinese Journal of Aeronautics*, Vol. 28, No. 2, 2015, pp. 545-555.
- [17] Chen, S.C., Yue, K.Z. and Hu, B., "Numerical Simulation on the RCS of Variable-sweep Wing Aircraft," *Journal of Aerospace Technology and Management*, Vol. 7, No. 2, 2015, pp. 170-178.
- [18] Yue, K.Z., Chen, S.C. and Shu, C.Y., "Calculation of Aircraft Target's Single-Pulse Detection Probability," *Journal of Aerospace Technology and Management*, Vol. 7, No. 3, 2015, pp. 314-322.
- [19] Yue, K.Z., Sun, C. and Ji, J.Z., "Numerical simulation on the stealth characteristics of twin-vertical-tails for fighter," *Journal of Beijing University of Aeronautics and Astronautics*, Vol. 40, No. 2, 2014, pp. 160-165.
- [20] Yue, K.Z., Jia, Z.H. and Ji, J.Z., "Numercal simulation on the RCS of carrier-based electronic warfare aircraft," *Systems Enginceering and Electronics*, Vol. 36, No. 5, 2014, pp.852-858.
- [21] Ruan, Y.Z., *Radar cross section and stealth technology*, National Defense Industry Press, Beijing, 1998, pp.99-120.
- [22] Yue, K.Z., Tian, Y.F., Liu, H. and Han, W., "Conceptual Design and RCS Property Research of Three-surface Strike Fighter," *International Journal of Aeronautical and Space Sciences*, \_Vol. 15, No. 3, 2014, pp. 309-319.